Deuterium Kinetic Isotope Effects and Their Temperature Dependence in the Gas-Phase S_N2 Reactions $X^- + CH_3Y \rightarrow CH_3X + Y^-$ (X, Y = Cl, Br, I)

Wei-Ping Hu and Donald G. Truhlar*

Contribution from the Department of Chemistry and Supercomputer Institute, University of Minnesota, Minneapolis, Minnesota 55455-0431

Received May 12, 1995[⊗]

Abstract: Extended-basis-set calculations with electron correlation have been carried out for the reactant and transition state properties of the gas-phase S_N2 reactions $Cl^- + CH_3Br \rightarrow CH_3Cl + Br^-$, $Cl^- + CH_3I \rightarrow CH_3Cl + I^-$, and $Br^- + CH_3I \rightarrow CH_3Br + I^-$. The resulting force fields are used for canonical unified statistical theory calculations of the rate constants of these reactions and their perdeuterated analogs. Kinetic isotope effects (KIEs) and their temperature dependences have been calculated and analyzed, and they are compared to available experimental data. We find only small deviations of the generalized transition state theory results from conventional transition state theory, and we obtain reasonable agreement (~10%) with experimental results for the KIEs of the first two reactions, but the KIEs that we predict for the third reaction are up to 26% higher than experiment.

Introduction

The bimolecular nucleophilic substitution (S_N2) reaction[1] is the most widely studied class of ion−molecule reaction in organic chemistry. Originally studied in condensed phases, in recent years the reaction has been extensively studied in the gas phase both theoretically[2] and experimentally.[3] However, some aspects of this type of reaction are not well understood; for example, the factors controlling kinetic isotope effects (KIEs) and their temperature dependences are still controversial. In the present work, we performed high-level electronic structure calculations on the reactants and the transition states of three S_N2 reactions involving a methyl halide and a halide ion, in particular, $Cl^- + CH_3Br \rightarrow CH_3Cl + Br^-$, $Cl^- + CH_3I \rightarrow CH_3Cl + I^-$, and $Br^- + CH_3I \rightarrow CH_3Br + I^-$. By using the data from the electronic structure calculations in dual-level[4,5] canonical unified statistical (CUS) theory[6-9] calculations, we calculated the low-pressure rate constants and kinetic isotope effects of all three reactions at 300 K and as functions of temperature. These calculations provide a fundamental test of theory and indeed, as discussed later in the paper, lead to a stimulating disagreement between theory and experiment for one of the reactions.

Theoretical Background

For many gas-phase S_N2 reactions, including all three studied here, the energies of the transition states are lower than the energies of the reactants, but by only a few kcal/mol. With such negative barrier heights, the rate constants show negative temperature dependences in a temperature range around room temperature.

The general shape of the potential energy function along the minimum energy path is illustrated in Figure 1. The potential function shows two wells, labeled C and C', corresponding to reactant and product ion-dipole complexes, respectively, on either side of a saddle point corresponding to transfer of the methyl group. In the present paper we calculate only the low-pressure bimolecular reaction rates. In the low-pressure limit molecules do not suffer any collisions with third bodies while they pass through the C, C', and transition state regions. Under such conditions, there are three possible locations for a dynamical bottleneck to reaction: (i) in the entrance channel, a bottleneck to formation of the reactant ion-dipole complex C, (ii) in the central barrier region, and (iii) in the exit channel between the product ion-dipole complex C' and asymptotic

[⊗] Abstract published in *Advance ACS Abstracts*, October 1, 1995.

(1) Reviews have been given by: (a) Riveros, J. M.; Jose, S. M.; Takashima, I. *Adv. Phys. Org. Chem.* **1985**, *21*, 197. (b) Shaik, S. S.; Schlegel, H. B.; Wolfe, S. *Theoretical Aspects of Physical Organic Chemistry: The S_N2 Mechanism*; John Wiley & Sons: New York, 1992. A search on S_N2 in the *Chemistry Citation Index* for 1992−4 turned up 364 references, so it is clear that activity in this area is continuing.

(2) Representative recent theoretical papers from which earlier work may be traced: (a) Wang, H. B.; Zhu, L.; Hase, W. L. *J. Phys. Chem.* **1994**, *98*, 1608. (b) Wang, H. B.; Peslherbe, G. H.; Hase, W. L. *J. Am. Chem. Soc.* **1994**, *116*, 9644. (c) Boyd, R. J.; Kim, C. K.; Shi, Z.; Weinberg, N.; Wolfe, S. *J. Am. Chem. Soc.* **1993**, *115*, 10147. (d) Poirier, R. A.; Wang, W. L.; Westaway, K. C. *J. Am. Chem. Soc.* **1994**, *116*, 2526. (e) Buhl, M.; Schaefer, H. F. *J. Am. Chem. Soc.* **1993**, *115*, 9143. (f) Shaik, S.; Ioffe, A.; Reddy, A. C.; Pross, A. *J. Am. Chem. Soc.* **1994**, *116*, 262. (g) Baj, S.; Dawid, M. *Theochem* **1994**, *112*, 67. (h) Anh, N. T.; Thanh, B. T.; Thao, H. H.; Nguessan, Y. T. *New J. Chem.* **1994**, *18*, 489. (i) Glad, S. S.; Jensen, F. *J. Chem. Soc., Perkin Trans. 2* **1994**, 871. (j) Hu, W.-P.; Truhlar, D. G. *J. Am. Chem. Soc.* **1994**, *116*, 7797. (k) Deng, L. Q.; Branchadell, V.; Ziegler, T. *J. Am. Chem. Soc.* **1994**, *116*, 10645. (l) Minyaev, R. M.; Wales, D. J. *J. Phys. Chem.* **1994**, *98*, 7942. (m) Glukhovtsev, M. N.; Pross, A.; Radom, L. *J. Am. Chem. Soc.* **1995**, *117*, 2024. (n) Lucchini, V.; Modena, G.; Pasquato, L. *J. Am. Chem. Soc.* **1995**, *117*, 2297.

(3) Recent work includes: (a) Gronert, S.; Depuy, C. H.; Bierbaum, V. M. *J. Am. Chem. Soc.* **1991**, *113*, 4009. (b) Viggiano, A. A.; Morris, R. A.; Paschkewitz, J. S.; Paulson, J. F. *J. Am. Chem. Soc.* **1992**, *114*, 10477. (c) Knighton, W. B.; Bognar, J. A.; O'Connor, P. M.; Grimsrud, E. P. *J. Am. Chem. Soc.* **1993**, *115*, 12079. (d) Wladkowski, B. D.; Wilbur, J. L.; Brauman, J. I. *J. Am. Chem. Soc.* **1994**, *116*, 2471. (e) Graul, S. T.; Bowers, M. T. *J. Am. Chem. Soc.* **1994**, *116*, 3875. (f) Cyr, D. M.; Scarton, M. G.; Wiberg, K. B.; Johnson, M. A.; Nonose, S.; Hirokawa, J.; Tanaka, H.; Kondow, T.; Morris, R. A.; Viggiano, A. A. *J. Am. Chem. Soc.* **1995**, *117*, 1828.

(4) Hu, W.-P.; Liu, Y.-P.; Truhlar, D. G. *J. Chem. Soc., Faraday Trans.* **1994**, *90*, 1715.

(5) Corchado, J. C.; Espinosa-Garcia, J.; Hu, W.-P.; Rossi, I.; Truhlar, D. G. *J. Phys. Chem.* **1995**, *99*, 687.

(6) Hirschfelder, J. O.; Wigner, E. *J. Chem. Phys.* **1939**, *7*, 616.

(7) (a) Garrett, B. C.; Truhlar, D. G. *J. Chem. Phys.* **1979**, *70*, 1593. (b) Truhlar, D. G.; Garrett, B. C. *Acc. Chem. Res.* **1980**, *13*, 440.

(8) (a) Miller, W. H. *J. Chem. Phys.* **1976**, *65*, 2216. (b) Garrett, B. C.; Truhlar, D. G. *J. Chem. Phys.* **1982**, *76*, 1853.

(9) Truhlar, D. G.; Isaacson, A. D.; Garrett, B. C. In *Theory of Chemical Reaction Dynamics*; Baer, M., Ed.; CRC Press; Boca Raton, 1985; Vol. 4, p 65.

0002-7863/95/1517-10726$09.00/0

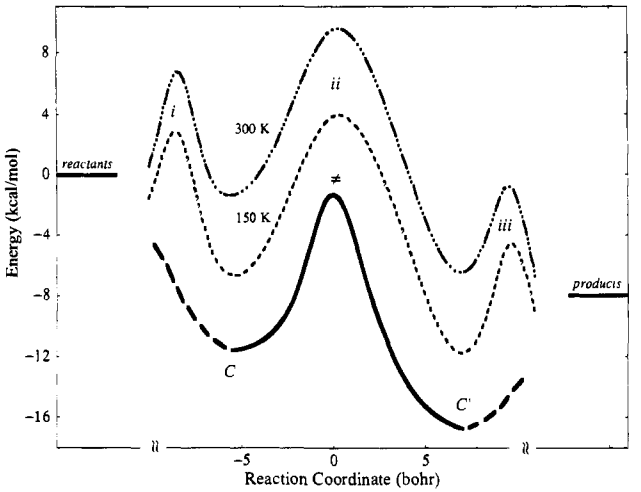

Figure 1. Shape of potential energy (the lowest curve) and standard-state generalized free energy of activation curves along the minimum energy path, illustrated for $Cl^- + CH_3Br \rightarrow CH_3Cl + Br^-$. The standard state is 1 Torr for an ideal gas. The reaction coordinate is measured in a mass-scaled Cartesian coordinate system[9] with a mass μ of 1 amu. The free energy values at stationary points and the potential energy curve in the region between C and C' (see text for notation) were calculated using the dual-level direct dynamics method with the MP2/PDZ+ high-level data and the AM1-SRP low-level surface. The generalized free energy activation values at i and iii were calculated by the ion-dipole capture approximation of Celli *et al.*[10] The rest of the generalized free energy activation curves, except at stationary points, are schematic.

products. The rate constants for passage through these bottleneck regions are labeled k_i, k_{ii}, and k_{iii}, and $k^C(T)$ and $k^{C'}(T)$ are the one-way flux rate constants evaluated at the ion-dipole minima. All these flux coefficients are for forward reaction of A + BC as if *i*, *ii*, *iii*, *C*, or *C'*, respectively, were the only transition state. The final reaction rate k is calculated by the canonical unified statistical (CUS) model as

$$k(T) = k_{ii}(T)\, R^{CUS}(T) \tag{1}$$

where[6-9]

$$R^{CUS}(T) = \left(\frac{k_{ii}(T)}{k_i(T)} - \frac{k_{ii}(T)}{k^C(T)} + 1 - \frac{k_{ii}(T)}{k^{C'}(T)} + \frac{k_{ii}(T)}{k_{iii}(T)}\right)^{-1} \tag{2}$$

The ion-molecule association rate constant, $k_i(T)$, is estimated based on the ion-dipole capture approximation of Celli *et al.*,[10] and the rate constant k_{iii} may be estimated from the capture rate of the products and the equilibrium constant for the reverse association reaction. Since these minima are usually about 10 kcal/mol or more deep, we make the reasonable approximations that $k_{ii}(T)/k^C(T) \ll 1$ and $k_{ii}(T)/k^{C'} \ll 1$, and we neglect the second and fourth terms in (2). Furthermore, $k_{iii}(T) \gg k_{ii}(T)$, so the fifth term is also neglected.

The rate coefficient $k_{ii}(T)$ is obtained by carrying out dual-level direct dynamics calculations of the canonical variational transition state theory (CVT)[7] rate constant. The high-level data are obtained from correlated *ab initio* electronic structure calculations as mentioned in the next section, and the low-level data are obtained by employing the NDDO-SRP[4,5,11] method.

We consider the reactions

$$X^- + CH_3Y \rightarrow CH_3X + Y^- \tag{R1}$$

$$X^- + CD_3Y \rightarrow CD_3X + Y^- \tag{R2}$$

where X and Y are halogen atoms. We define the KIE to be the ratio of the rate constant (k_H) of R1 to the rate constant (k_D) of R2. The KIE of the canonical unified statistical theory can be factored[2j,11,12] as

$$\mathrm{KIE} = \eta_{trans}\eta^{\ddagger}_{rot}\eta^{\ddagger}_{vib}\eta_{var}\eta_{cap} \tag{3}$$

where the first three factors refer to contributions from translational, rotational, and vibrational motions, respectively, with $\eta^{\ddagger}_{rot}$ and $\eta^{\ddagger}_{vib}$ evaluated at the conventional transition state. The fourth factor is the contribution from variational effects[7] and is defined as:

$$\eta_{var} = \frac{k_D^{TST}k_H^{CVT}}{k_H^{TST}k_D^{CVT}} \tag{4}$$

where k^{TST} and k^{CVT} are the conventional transition state theory (TST)[9] rate constant and CVT rate constant, respectively. The last factor comes from the capture rate contribution to eq 2, i.e.,

$$\eta_{cap} = R_H^{CUS}/R_D^{CUS} \tag{5}$$

From transition state theory and quantum statistics, we have

$$\eta_{trans} = (\mu_{rel,D}/\mu_{rel,H})^{3/2} \tag{6}$$

where μ_{rel} is the reduced mass of relative translational motion of the reactants, and with a classical treatment of rotations, we have

$$\eta^{\ddagger}_{rot} = \left[\frac{(\det \mathbf{I})^{\ddagger}_H(\det \mathbf{I})^{R}_D}{(\det \mathbf{I})^{\ddagger}_D(\det \mathbf{I})^{R}_H}\right]^{1/2} \tag{7}$$

where det **I** is the determinant of the moment of inertia tensor, a superscript ‡ means transition state, a superscript R means reactant, which is CH_3Y or CD_3Y in this study, a subscript H refers to the species containing protium, and a subscript D refers to the species containing deuterium. The vibrational contribution can be written as

$$\eta^{\ddagger}_{vib} = \frac{q^{\ddagger}_{vib,H}\, q^{R}_{vib,D}}{q^{\ddagger}_{vib,D}\, q^{R}_{vib,H}} \tag{8}$$

where q_{vib} is the vibrational partition function (with classical zero of energy, as opposed to zero point level as the zero of energy). The vibrational contribution can be further factored into contributions from low-, mid-, and high-frequency modes

$$\eta^{\ddagger}_{vib} = \eta^{\ddagger}_{low}\eta^{\ddagger}_{mid}\eta^{\ddagger}_{high} \tag{9}$$

The expressions for these contributions are similar to eq 8 but only include the frequencies in particular ranges. The value of the classical barrier height cancels out in the conventional transition state theory KIE, but it does affect η_{var}.

From eqs 6 and 7 we see that the translational and rotational contributions are temperature independent and that the temper-

(10) Celli, F.; Weddle G.; Ridge, D. P. *J. Chem. Phys.* **1980**, *73*, 801.
(11) González-Lafont, A.; Truong, T. N.; Truhlar, D. G. *J. Phys. Chem.* **1991**, *95*, 4618.
(12) (a) Garrett, B. C.; Truhlar, D. G.; Magnuson, A. W. *J. Chem. Phys.* **1982**, *76*, 2321. (b) Tucker, S. C.; Truhlar, D. G.; Garrett, B. C.; Isaacson, A. D. *J. Chem. Phys.* **1985**, *82*, 4102. (c) Lu, D.-h.; Maurice, D.; Truhlar, D. G. *J. Am. Chem. Soc.* **1990**, *112*, 6206. (d) Zhao, X. G.; Lu, D.-h.; Liu, Y.-P.; Lynch, G. C.; Truhlar, D. G. *J. Chem. Phys.* **1992**, *97*, 6369.

ature dependence of the KIE in eq 3 arises solely from the vibrational, variational, and capture contributions. As we will see, the translational and variational contributions are very close to unity, the rotational contributions in these reactions are "normal" (larger than unity), and the vibrational contributions η_{vib} are "inverse" (less than unity).

As a final item of background we summarize the assumptions of the three levels of dynamical theory most relevant to the present calculations. Conventional TST assumes that a phase space dividing surface through the saddle point provides a perfect dynamical bottleneck. In classical language this means that trajectories passing through such a dividing surface in the direction of products originated at reactants and inevitably proceed to products without returning to the dividing surface, i.e., that trajectories do not recross the bottleneck dividing surface.[13] In quantum mechanical language it means that the transmission coefficients of all quantized levels of the transition state are unity.[14] CVT again presupposes a single dynamical bottleneck with no recrossing trajectories (classical language) or with unit transmission coefficients (quantal language), but it does not require the dynamical bottleneck to be located at the saddle point, and furthermore it allows the bottleneck location to depend on temperature.[7,9] The present systems challenge the assumptions of these theories by the possibility that there is significant recrossing of even the best single bottleneck dividing surface, due, for example, to trapping in the ion-dipole complex regions, which would facilitate turning the trajectories back toward the direction from which they came. CUS theory is the simplest way to take account of a complex region between two dynamical bottlenecks.

CVT is an attempt to correct for recrossing of the saddle point dynamical bottleneck by finding a better dynamical bottleneck. The unified statistical theory[8] is an attempt to take account for multiple bottleneck regions, and it is based on the branching analysis of Hirschfelder and Wigner,[6] which may also be derived as the least-biased estimate (the estimate with maximal information theoretic entropy) of the reaction rate constant consistent with the fluxes through the individual bottlenecks and with the conservation of flux.[15] In the final analysis, the reader should be aware that the unified statistical method does not necessarily account for all the factors that could lead to recrossing, nor should it be considered to provide a bound from either direction on the magnitude of recrossing effects.[16] It is necessary to include true dynamics (i.e., more than local fluxes through various dividing surfaces) to estimate recrossing reliably; when quantization constraints are unimportant that can be accomplished by running classical or quasiclassical trajectories, but quantization constraints are very significant for thermal rate constants. One indication of this is the sheer magnitude of the zero point energy at the saddle point, e.g., 23.5 kcal/mol for $ClCH_3Br^-$; another is the fact that variational transition state theory is much more accurate in a quantal world than in a classical one.[17] One possible way to include both recrossing and quantization constraints is called the unified dynamical theory,[9,18] but that would not include quantum effects on energy mixing in the complex region; anyway it is beyond our scope to discuss that further here.

For the reaction dynamics at the central barrier, we would not expect much difference in conclusions if we used microcanonical variational theory instead of canonical or if we took explicit account of conservation of total angular momentum.

Su *et al.*[19] have discussed orientation effects on the capture rate, but these are not considered here.

Computational Methods

The data needed for the calculation of k_i consist of dipole moments and polarizabilities of the neutral reactants. The dipole moments[20] and the polarizabilities[20] used to calculate k_i are 1.81 D and 5.87×10^{-24} cm^3 for CH_3Br and 1.62 D and 7.97×10^{-24} cm^3 for CH_3I.

Dual-level canonical variational transition state theory (CVT) rate constant calculations for $k_{ii}(T)$ were carried out with version 6.5 of the MORATE[21] program using methods explained in detail in a previous paper.[4] In the dynamics calculations, unless otherwise stated, all vibrations were treated harmonically. High-level data for moments of inertia and vibrational frequencies were obtained from *ab initio* calculations as described in later paragraphs of this section; the high-level barrier heights were inferred from experiment by adjusting the classical barrier heights used in the dual-level CVT rate constant calculations for k_{ii} until the calculated CUS rate constants (using eqs 1 and 2) at 300 K agreed with the experimental values in refs 3a and 3b; and the low-level data for the CVT part of the CUS calculations were based on NDDO-SRP semiempirical methods. These SRP methods are based either on the AM1[22] or PM3[23] method, and they are fitted to reproduce the experimental reaction energetics. (See the supporting information for the SRP parameters.)

For the high-level calculations, geometries needed for calculating moments of inertia and force fields needed for calculating vibrational partition functions were obtained by electronic structure calculations. Two consistent sets of calculations are presented for the barrier height, reactant frequencies, and transition state frequencies of each reaction in this chapter, and for two of the reactions we also present another calculation. In the first set of calculations applied to all three reactions, the basis sets used for hydrogen, carbon, and chlorine are Dunning and Woon's augmented correlation consistent polarized valence double-ζ (aug-cc-pVDZ) sets.[24] For bromine we used Wadt and Hay's[25] effective core potential (ECP) to represent the core electrons, and we used an uncontracted basis set consisting of Wadt and Hay's[25] 3s3p valence basis augmented with a d polarization function set (with exponent 0.384) and diffuse s, p, and d functions (with exponents 0.0635, 0.0459, and 0.128, respectively) for the bromine valence electrons. For iodine we used the effective core potential and basis set denoted as the ECP set in a previous paper,[26] which gives full details. In the rest of this chapter we call the basis sets used in this set of calculations the PDZ+ set.

In the second set of calculations applied to all three reactions, the basis sets used for hydrogen, carbon, and chlorine are Dunning and Woon's augmented correlation consistent polarized valence triple-ζ (aug-cc-pVTZ) sets[24] without diffuse d and f functions. The basis sets used for bromine and iodine are the same as in the first set of calculations except a set of polarized f functions are added to the valence basis set with exponents of 0.60 and 0.52 for bromine and iodine, respectively. In the rest of this paper we call the basis sets used in this set of calculations the PTZ+ set. The number of contracted Gaussian basis functions and primitive Gaussian basis functions in

(13) (a) Wigner, E. *Trans. Faraday Soc.* **1938**, *34*, 29. (b) Pechukas, P. *Ber. Bunsenges. Phys. Chem.* **1982**, *86*, 372.

(14) Chatfield, D. C.; Friedman, R. S.; Schwenke, D. W.; Truhlar, D. G. *J. Phys. Chem.* **1992**, *96*, 2414.

(15) Pollak, E.; Levine, R. D. *Ber. Bunsenges. Phys. Chem.* **1982**, *86*, 458.

(16) Garrett, B. C.; Truhlar, D. G. *J. Chem. Phys.* **1982**, *76*, 1853.

(17) Truhlar, D. G.; Isaacson, A. D.; Skodje, R. T.; Garrett, B. C. *J. Phys. Chem.* **1982**, *86*, 2252.

(18) Truhlar, D. G.; Garrett, B. C. *Faraday Discuss. Chem. Soc.* **1987**, *84*, 464.

(19) Su, T.; Morris, R. A.; Viggiano, A. A.; Paulson, J. F. *J. Phys. Chem.* **1990**, *94*, 8426.

(20) Lide D. R., Ed. *Handbook of Chemistry and Physics*, 71st ed; CRC Press; Boca Raton, 1990.

(21) Hu, W.-P.; Lynch, G. C.; Liu, Y.-P.; Rossi, I.; Stewart, J. J. P.; Steckler, R.; Garrett, B. C.; Isaacson, A. D.; Lu, D.-h.; Melissas, V. S.; Truhlar, D. G., MORATE Version 6.5. *QCPE Bull.* **1995**, *15*, 26.

(22) (a) Dewar, M. J. S.; Zoebisch, E. G.; Healy, E. F.; Stewart, J. J. P. *J. Am. Chem. Soc.* **1985**, *107*, 3902. (b) Dewar, M. J. S.; Zoebisch, E. G. *J. Mol. Struct. (THEOCHEM)* **1988**, *180*, 1.

(23) Stewart, J. J. P. *J. Comput. Chem.* **1989**, *10*, 221.

(24) (a) Dunning, T. H., Jr. *J. Chem. Phys.* **1989**, *90*, 1007. (b) Woon, D. E.; Dunning, T. H., Jr. *J. Chem. Phys.* **1993**, *98*, 1358.

(25) Wadt, W. R.; Hay, P. J. *J. Chem. Phys.* **1985**, *82*, 284.

(26) Hu, W.-P.; Truhlar, D. G. *J. Phys. Chem.* **1994**, *98*, 1049.

Table 1. Calculated Geometries[a] of Reactants and Products (CH_3Y)

	CH_3Cl	CH_3Br	CH_3I
R_{C-Y}, Å	1.797[b]	1.955	2.146
	1.781[c]	1.938	2.118
	(1.780)[d]	(1.936)	(2.139)
R_{C-H}, Å	1.096	1.096	1.096
	1.083	1.083	1.083
	(1.097)	(1.090)	(1.092)
∠Y−C−H, deg	108.23	107.91	107.78
	108.51	108.10	108.09
	(107.35)	(107.07)	(106.67)

[a] All structures have C_{3v} symmetry. [b] Upper values calculated at the MP2/PDZ+ level. [c] Lower values calculated at the MP2/PTZ+ level. [d] Values in parentheses are experimental values from ref 30.

the PTZ+ basis set are 159 and 291 for $Cl^- + CH_3Br$ and $Cl^- + CH_3I$ and 154 and 196 for $Br^- + CH_3I$, respectively.

All the high-level geometry optimization and frequency calculations include electron correlation, and for the two sets of calculations just discussed, this was carried out at the second-order perturbation theory level of Møller and Plesset (MP2).[27] The core electrons were not correlated in any calculation. The transition states were optimized using the eigenvector-following (EF) algorithm.[28] The electronic structure calculations were carried out with the GAUSSIAN 92[29] program on the Cray C90 computer at Minnesota Supercomputer Institute.

Geometry optimization and frequency calculations have also been performed at the MP2 level for all three methyl halides and for the saddle point of $Cl^- + CH_3Br$ with the full aug-cc-pVTZ basis set on C, H, and Cl, and with the PTZ+ sets on Br and I augmented by an additional set of f diffuse functions (exponents 0.2 and 0.173 for Br and I, respectively). This basis is denoted PTZ++ set in the rest of this paper. The detailed geometry and frequency data of this calculation are presented in the supporting information. Calculations were also performed at the MP4[27] level with the PDZ+ basis set on the reactants and saddle point of $Br^- + CH_3I$. The geometry data are presented in the supporting information. The PTZ++ and MP4 calculations serve as convergence checks. Many additional calculations at other levels of electronic structure theory are presented in the supporting information.

Results

Structure and Energetics. Table 1 gives the calculated and experimental[30] geometries of the three methyl halides. Table 2 lists the calculated geometries of the transition states of the three reactions. The calculated and experimental[31] harmonic vibrational frequencies of the methyl halides are listed in Table 3. The calculated harmonic vibrational frequencies of the transition states are listed in Table 4. Table 5 gives the calculated and experimental[32] exoergicities and barrier heights.

Table 2. Calculated Geometries[a] of Transition States ($X-CH_3-Y^-$)

	$Cl-CH_3-Br^-$		$Cl-CH_3-I^-$		$Br-CH_3-I^-$	
	value	change[b]	value	change	value	change
R_{C-Y}, Å	2.430[c]	0.475	2.587	0.441	2.623	0.477
	2.392[d]	0.454	2.552	0.434	2.594	0.476
R_{C-H}, Å	1.082	−0.014	1.083	−0.013	1.083	−0.013
	1.069	−0.014	1.070	−0.013	1.070	−0.013
R_{C-X}, Å	2.351		2.387		2.501	
	2.322		2.350		2.460	
∠Y−C−H, deg	91.08	−17.15	92.06	−15.85	90.97	−16.81
	91.28	−17.23	92.13	−15.96	90.81	−17.28

[a] All structures have C_{3v} symmetry. [b] Change from the reactant. [c] Upper values calculated at the MP2/PDZ+ level. [d] Lower values calculated at the MP2/PTZ+ level.

Table 3. Calculated and Experimental Harmonic Vibrational Frequencies (in cm^{-1}) of CH_3Y and CD_3Y

	CH_3Cl	CD_3Cl	CH_3Br	CD_3Br	CH_3I	CD_{3I}
ν_1 (a_1)	3105[a]	2221	3108	2222	3108 (3071)	2221 (2194)
	3116[b]	2229	3119	2231	3117	2229
	[3062]	[2207]	[3061]	[2196]	[3060]	[2210]
ν_2 (a_1)	1368	1034	1325	1003	1282 (1272)	970 (962)
	1398	1059	1350	1024	1310	994
	[1398]	[1054]	[1332]	[1002]	[1288]	[975]
ν_3 (a_1)	750	715	625	588	547 (526)	512 (493)
	766	728	651	610	577	538
	[733]	[696]	[614]	[580]	[533]	[502]
ν_4 (e)	3225	2394	3233	2400	3235 (3192)	2401 (2370)
	3227	2396	3235	2402	3234	2401
	[3209]	[2379]	[3213]	[2381]	[3229]	[2400]
ν_5 (e)	1473	1066	1465	1061	1458 (1449)	1056 (1051)
	1504	1088	1492	1080	1485	1076
	[1520]	[1092]	[1506]	[1084]	[1504]	[1083]
ν_6 (e)	1033	776	968	721	902 (888)	669 (659)
	1044	785	980	731	916	680
	[1049]	[750]	[975]	[730]	[906]	[676]

[a] Upper values calculated at the MP2/PDZ+ level with values in parentheses at the MP4/PDZ+ level. [b] Lower values calculated at the MP2/PTZ+ level. [c] Values in brackets are experimental values from ref 31.

In Table 5 the directly calculated classical barrier heights are listed in the "calc" column, and the barrier heights inferred from experiments are listed in the "expt" column.

Room Temperature Rates. Table 6 gives the calculated values of k_i, k_{ii}, and R^{CUS} at 300 K. It also gives the experimental rate constant k at 300 K that was used in the empirical determination of the experimental barrier height as explained above.

We calculated the KIEs of all three reactions, and the results are compared with the experimental[3a,b] values in Table 7. Table 8 shows the results of a factor analysis of the KIEs at 300 K.

Temperature Dependence of Rates. Figures 2−4 show the temperature dependence of the calculated rate constants and KIEs of the three reactions under study. Figure 5 shows the k_{ii} and k for $Cl^- + CH_3I$ as a function of temperature. For the other two reactions, k_{ii} and k are almost identical. Results of the factor analysis of the vibrational contributions to the KIEs and the η_{cap} in the temperature range 200−1000 K are shown in Figures 6−8.

Discussion

Geometries. The calculated values of the methyl halide geometries (Table 1) are in good agreement with the values derived from rotational spectroscopy;[30] in particular the carbon−halogen bond lengths are all within 0.021 Å of the experimental data, the carbon-hydrogen bond lengths are within 0.006 Å for the MP2/PDZ+ calculations and within 0.014 Å for the MP2/

(27) (a) Hehre, W. J.; Radom, L.; Schleyer, P. v. R.; Pople, J. A. *Ab initio Molecular Orbital Theory*; Wiley: New York, 1986. (b) Adams, G. F.; Bent, G. D.; Bartlett, R. J.; Purvis, G. D. In *Potential Energy Surfaces and Dynamics Calculations*; Truhlar, D. G., Ed.; Plenum: New York, 1981; p 133.

(28) (a) Cerjan, C. J.; Miller, W. H. *J. Chem. Phys.* **1981**, *75*, 2800. (b) Simons, J.; Jorgenson, P.; Taylor, H.; Ozment, J. *J. Phys. Chem.* **1983**, *87*, 2745. (c) Banerjee, A.; Adams, N.; Simons, J.; Shepard, R. *J. Phys. Chem.* **1985**, *89*, 52.

(29) Gaussian 92, Revision D.2, Frisch, M. J.; Trucks, G. W.; Head-Gordon, M.; Gill, P. M.; Wong, M. W.; Foresman, J. B.; Johnson, B. G.; Schlegel, H. B.; Robb, M. A.; Replogle, E. S.; Gomperts, R.; Andres, J. L.; Raghavachari, K.; Binkley, J. S.; Gonzalez, C.; Martin, R. L.; Fox, D. J.; Defrees, D. J.; Baker, J.; Stewart, J. J. P.; Pople, J. A.; Gaussian, Inc.: Pittsburgh, PA, 1992.

(30) Chang, T.-S. Ph.D. Thesis, University of Michigan, 1954, as quoted in: King W. T.; Mills, I. M.; Crawford, B., Jr. *J. Chem. Phys.* **1957**, *27*, 455.

(31) Dickson, A. D.; Mills, I. M.; Crawford, B., Jr. *J. Chem. Phys.* **1957**, *27*, 445.

(32) Chase, M. W., Jr.; Davies, C. A.; Downey, J. R., Jr.; Frurip, D. J.; McDonald, R. A.; Syverud, A. N. *J. Phys. Chem. Ref. Data* **1985**, *14*, Suppl. 1.

Table 4. Calculated Harmonic Vibrational Frequencies (in cm^{-1}) of Transition States

	$Cl-CH_3-Br^-$	$Cl-CD_3-Br^-$	$Cl-CH_3-I^-$	$Cl-CD_3-I^-$	$Br-CH_3-I^-$	$Br-CD_3-I^-$
ν_1 (a_1)	3213[a]	2273	3207	2269	3205 (3167)	2267 (2240)
	3225[b]	2282	3221	2279	3219	2277
ν_2 (a_1)	1037	743	993	711	957 (929)	682 (662)
	1029	738	989	708	958	682
ν_3 (a_1)	188	187	170	169	127 (123)	127 (123)
	195	195	175	175	130	130
ν_4 (e)	3429	2560	3422	2555	3421 (3376)	2553 (2519)
	3430	2561	3425	2557	3423	2555
ν_5 (e)	1405	1035	1402	1032	1401 (1391)	1031 (1024)
	1426	1050	1426	1049	1426	1050
ν_6 (e)	941	667	913	647	900 (864)	637 (612)
	955	677	929	659	922	653
ν_7 (e)	190	175	170	161	161 (155)	148 (142)
	199	183	182	168	168	154
ν_i[c]	464*i*	464*i*	442*i*	442*i*	425*i* (389*i*)	424*i* (389*i*)
	490*i*	490*i*	474*i*	474*i*	457*i*	457*i*

[a] Upper values calculated at the MP2/PDZ+ level with values in parentheses at the MP4/PDZ+ level. [b] Lower values calculated at the MP2/PTZ+ level. [c] Imaginary frequency of the transition state.

Table 5. MP2 Calculations of Energies[a] of Reaction and Classical Barrier Heights (in kcal/mol)[b]

	ΔE		$V^{\ddagger}$	
reaction	calc	expt[c]	calc	expt[d]
$Cl^- + CH_3Br$	−6.7[e]	−8.0	−1.7	−1.3[g]
	−8.6[f]		−1.0	−1.3[h]
$Cl^- + CH_3I$	−12.2	−13.9	−4.2	−2.7
	−13.5		−2.7	−2.7
$Br^- + CH_3I$	−5.5	−5.9	−1.9	−1.4
	−4.8		0.6	−1.4

[a] Born−Oppenheimer energies, i.e., excluding zero point and thermal contributions. [b] Negative values of ΔE denote that the reaction is exoergic, and $V^{\ddagger}$ is the barrier height with respect to reactants. [c] Calculated from ΔH°_0 of ref 32 and harmonic frequencies of ref 31. [d] This quantity is the adjusted barrier height (used in calculating k_{ii}), which is obtained by fitting the calculated rate constant (eq 1) to the experimental rate constants of refs 3a (for the second the third reactions) and 3b (for the first reaction) at 300 K with the calculated frequency and moment-of-inertia information. [e] Upper entry: MP2/PDZ+ result. [f] Lower entry: MP2/PTZ+ result. [g] Upper entry: inferred from experimental rate constants and from MP2/PDZ+ frequencies and moments of inertia. [h] Lower entry: inferred from experimental rate constants and from MP2/PTZ+ frequencies and moments of inertia.

Table 6. Rate Constants (in cm^3 $molecule^{-1}$ s^{-1}) and R^{CUS} Factors at 300 K

reaction	k_i	k_{ii}	R^{CUS}	k
$Cl^- + CH_3Br$	2.35×10^{-9}	2.39×10^{-11}	0.99	2.4×10^{-11} [a]
$Cl^- + CD_3Br$	2.34×10^{-9}	2.62×10^{-11} [b]	0.99 [c]	2.7×10^{-11} [a]
		2.55×10^{-11} [b]	0.99 [c]	
$Cl^- + CH_3I$	2.16×10^{-9}	1.80×10^{-10}	0.92	1.7×10^{-10} [d]
$Cl^- + CD_3I$	2.15×10^{-9}	2.02×10^{-10} [b]	0.91 [c]	2.0×10^{-10} [d]
		1.99×10^{-10} [b]	0.92 [c]	
$Br^- + CH_3I$	1.60×10^{-9}	2.94×10^{-11}	0.98	2.9×10^{-11} [d]
$Br^- + CD_3I$	1.60×10^{-9}	3.19×10^{-11} [b]	0.98 [c]	3.8×10^{-11} [d]
		3.19×10^{-11} [b]	0.98 [c]	

[a] Experimental value from ref 3b. [b] k_{ii} for the perdeuterated reaction is calculated using the adjusted classical barrier height in Table 5. The upper value is obtained using the MP2/PDZ+ data, and the lower value is obtained using the MP2/PTZ+ data. [c] The upper value is obtained using the MP2/PDZ+ data, and the lower value is obtained using the MP2/PTZ+ data. [d] Experimental value from ref 3a.

PTZ+ calculations. (It is our experience that the C−H bond length is always about 0.01−0.015 Å too short at the MP2 level when using the correlation consistent triple-ζ basis set.) The halogen−carbon−hydrogen bond angles are within 1.1° of the experimental data. Table 2 shows that the carbon−hydrogen bonds in the transition states are shorter by about 0.013−0.014 Å than in the reactants in both calculations, and the halogen−carbon−hydrogen bond angles are all close to 90°, i.e., the methyl groups are almost planar in the transition states. For all these reactions, the making C−X bond is 0.54−0.59 Å longer than the product C−X bond, and the breaking C−Y bond is 0.43−0.48 Å longer than the reactant C−Y bond.

Table 7. Calculated and Experimental Kinetic Isotope Effects (KIEs) at 300 K

reaction	expt	level	calc
$Cl^- + CH_3Br$	0.88,[a] 0.80[b]	MP2/PDZ+	0.91
		MP2/PTZ+	0.94
		MP2/PTZ++	0.95
$Cl^- + CH_3I$	0.84[b]	MP2/PDZ+	0.90
		MP2/PTZ+	0.91
$Br^- + CH_3I$	0.76[b]	MP2/PDZ+	0.93
		MP2/PTZ+	0.93
		MP4/PDZ+	0.96

[a] From ref 3b. [b] From ref 3a.

Table 8. Factor[a,b] Analysis of the KIEs at 300 K

reaction	Level	η_{trans}	$\eta^{\neq}_{rot}$	η_{cap}	$\eta^{\neq}_{low}$	$\eta^{\neq}_{mid}$	$\eta^{\neq}_{high}$
$Cl^- + CH_3Br$	MP2/PDZ+	1.01	1.23	1.00	0.84	1.18	0.74
	MP2/PTZ+	1.01	1.23	1.00	0.84	1.21	0.74
	MP2/PTZ++	1.01	1.23	1.00	0.84	1.22	0.74
$Cl^- + CH_3I$	MP2/PDZ+	1.01	1.23	1.01	0.84	1.14	0.75
	MP2/PTZ+	1.01	1.23	1.00	0.84	1.17	0.74
$Br^- + CH_3I$	MP2/PDZ+	1.01	1.24	1.00	0.83	1.17	0.75
	MP2/PTZ+	1.01	1.24	1.00	0.83	1.19	0.75
	MP4/PDZ+	1.01	1.24	1.00	0.83	1.22	0.75

[a] η_{var} is unity to three significant figures (1.00) in all calculations. [b] Low denotes contributions from modes with $\nu_i < 300$ cm^{-1}; high denotes contributions from modes with $\nu_i > 2000$ cm^{-1}; and mid denotes the remaining contributions from the middle frequencies.

Frequencies. Table 4 shows excellent convergence of all transition state frequencies with respect to the size of the one-electron basis set. Our earlier modeling, mostly unpublished, led to variations (between various semiempirical SRP models and various levels of *ab initio* theory) in some of the frequencies (especially ν_2 and ν_6) by up to a hundred wave numbers, but the convergence in Table 4 is much better than this.

In assessing convergence of electron structure calculations, the reader should keep in mind that two types of convergence are important: size of the one-electron basis set (e.g., PDZ+, PTZ+) and level of electron correlation [e.g., MP2, MP4, CCSD(T)].

Energetics. The calculated energies of reaction (Table 5) are all close to the experimental values with the differences ranging from 1.7 to 0.4 kcal/mol for the MP2/PDZ+ calculation and from 1.1 to 0.4 kcal/mol for the MP2/PTZ+ calculation.

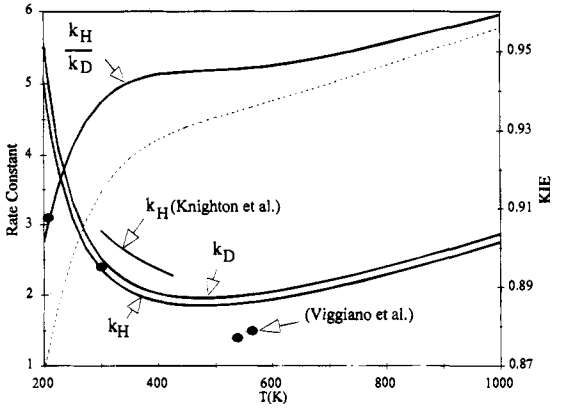

Figure 2. Rate constants (in 10^{-11} cm^3 molecule^{-1} s^{-1}) and KIEs for $Cl^- + CH_3Br$ and $Cl^- + CD_3Br$ reactions as a function of temperature. Results from the calculations using MP2/PTZ+ high-level data were used in plotting all solid curves in Figures 2–8. The dotted line in this figure is k_H/k_D calculated using MP2/PDZ+ high-level data. Experimental k_H data from the low-pressure experiments of refs 3c and 27 are also included.

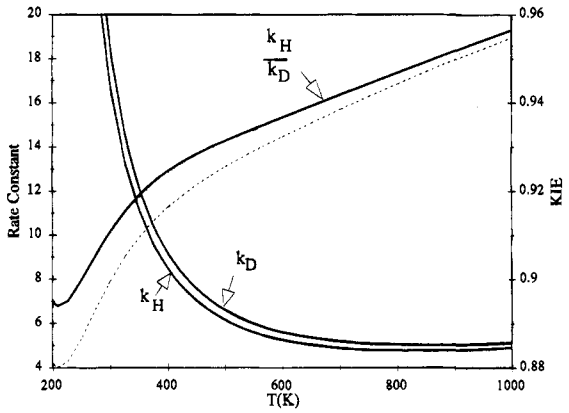

Figure 3. Rate constants (in 10^{-11} cm^3 molecule^{-1} s^{-1}) and KIEs for $Cl^- + CH_3I$ and $Cl^- + CD_3I$ reactions as a function of temperature. The solid curves are all based on the MP2/PTZ+ level. The dotted line is k_H/k_D calculated using MP2/PDZ+ high-level data.

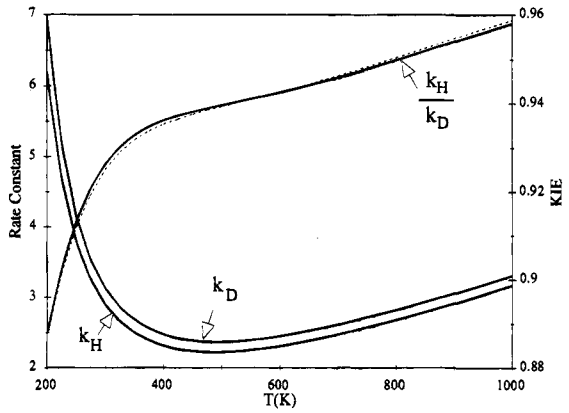

Figure 4. Rate constants (in 10^{-11} cm^3 molecule^{-1} s^{-1}) and KIEs for $Br^- + CH_3I$ and $Br^- + CD_3I$ reactions as a function of temperature. The solid curves are all based on the MP2/PTZ+ level. The dotted line is k_H/k_D calculated using MP2/PDZ+ high-level data.

The present calculated and inferred experimental barrier heights for $Cl^- + CH_3Br$ can be compared to the recent calculations of Wang *et al.*,[2a] with a less extended basis set. They calculated $V^{\ddagger} = -2.9$ kcal/mol with a combined SV4PP[33] /6-31G* [29] basis set at the Hartree–Fock[29] level, and they calculated −6.0 kcal/mol at the MP4//HF[29] level, where X//Y means that the energy is calculated at level X but with the geometry optimized at lower level Y. (Our own calculations in this paper do not employ the // technique; in all cases results at stationary points are based on optimized geometries for the correlation level and basis indicated.) We are in better agreement with previous work for the empirical classical barrier height: Viggiano *et al.*[34] estimated −1.5 kcal/mol, Wang *et al.*[2a] estimated −2.0 kcal/mol, and the present estimate is −1.3 kcal/mol.

Since the calculations reproduce the temperature dependence of the rate constants only within a factor of 1.3 from 300 to 564 K, it is hard to know which temperature is best to use to estimate the Born–Oppenheimer barrier height $V^{\ddagger}$. As stated

(33) Andzelm, J.; Klobukowski, M.; Radzio-Andzelm, E. *J. Comput. Chem.* **1984**, *5*, 146.

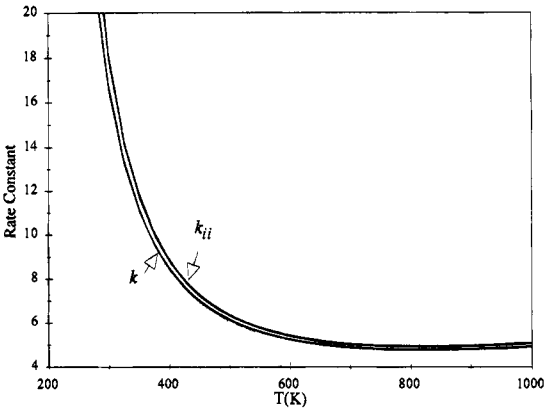

Figure 5. k and k_{ii} for the $Cl^- + CH_3I$ reaction as a function of temperature.

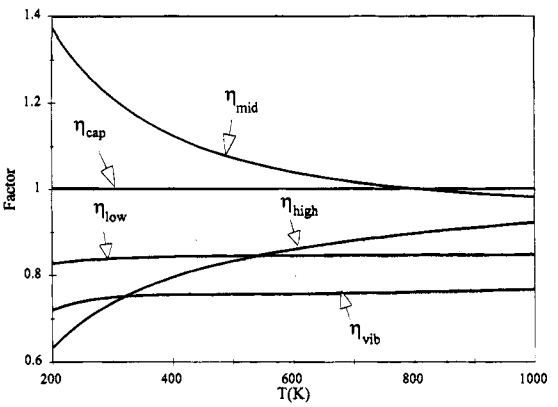

Figure 6. Factor analysis of the vibrational and capture rate contributions to the KIE of the $Cl^- + CH_3Br$ reaction as a function of temperature.

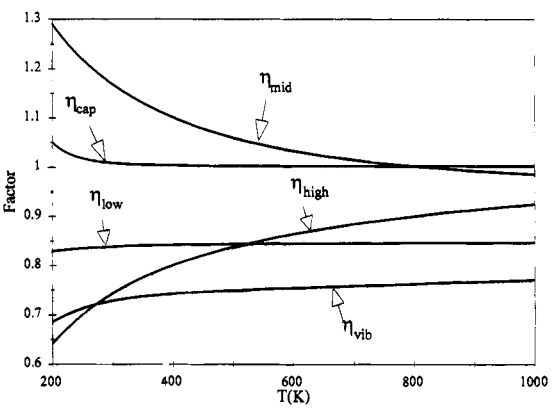

Figure 7. Factor analysis of the vibrational and capture rate contributions to the KIE of the $Cl^- + CH_3I$ reaction as a function of temperature.

(34) Viggiano, A. A.; Paschkewitz, J. S.; Morris, R. A.; Paulson, J. F.; González-Lafont, A.; Truhlar, D. G. *J. Am. Chem Soc.* **1991**, *113*, 9404.

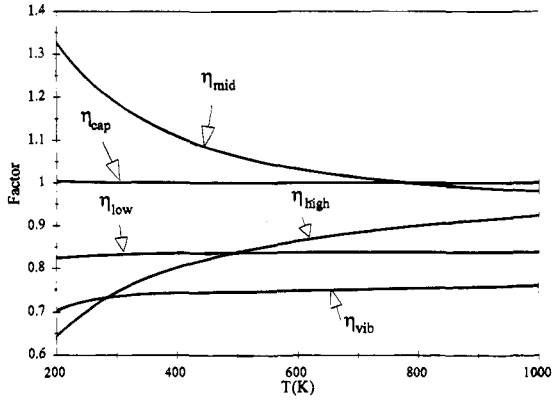

Figure 8. Factor analysis of the vibrational and capture rate contributions to the KIE of the $Br^- + CH_3I$ reaction as a function of temperature.

above, using the data of Viggiano *et al.* for 300 K yields $V^{\ddagger} = -1.3$ kcal/mol. We believe that the experimental rate constant at 300 K is more reliable because consistent values have been obtained in several recent measurements.[3b] If instead we used Viggiano *et al.*'s rate constant at 538 K, we would obtain -1.0 kcal/mol, but this would be less accurate if recrossing effects increase with T. Using 207 K leads to $V^{\ddagger} = -1.1$ kcal/mol.

Knighton *et al.*[3c] obtained the experimental rate constants at a higher pressure of 3 Torr. Their rate constants are about 20% higher at 300 K than the rate constants measured by Viggiano[3b] *et al.* at a pressure of 0.5 Torr. If Knighton *et al.*'s rate constant at 300 K (2.9×10^{-11} cm^3 molecule^{-1} s^{-1}) is used in our empirical fitting procedure, the empirical barrier height obtained is -1.4 kcal/mol. The results of Knighton *et al.* are discussed further below.

Rates. Table 6 shows that the R^{CUS} factors are very close to unity for $Cl^- + CH_3Br$ and $Br^- + CH_3I$ at 300 K, and so the calculated rate constants are close to k_{ii}. In fact, in the temperature range 200−1000 K the differences between calculated k_{ii} and k are all within 3% for these two reactions. The R^{CUS} factor is smaller for $Cl^- + CH_3I$ because of the much greater reaction efficiency compared to the other two reactions.

Knighton *et al.*[3c] found experimentally that rate constants at 308−423 K are factors of 1.4−2.0 larger at 640 Torr than at 3 Torr, where the latter pressure is more typical of the low-pressure conditions in most previous experiments. The experiments are difficult and have not been repeated yet. The increase in the rate at high pressure was interpreted[3c] as evidence for a pressure dependence of branching fractions of the reactants and products of the unimolecular decay of the intermediate reactant complex or of the transmission coefficient at the central barrier. Under reasonable additional assumptions, this could imply that either the low-pressure rate constant, the high-pressure one, or both cannot be treated by equilibrium rate theory, and Knighton *et al.* assumed based on evidence about energy utilization and disposal (see below) and trajectory findings concerning energy randomization in the complex that the low-pressure rates could not be so treated.

Indications of a breakdown of transition state theory are present in the trajectory calculation of Hase and co-workers.[2b] Two aspects of these calculations are especially relevant. First the unimolecular decay of ion-dipole complexes showed evidence for incomplete equilibration prior to decomposition. Second, in a finding which is more directly relevant to the present study, they found trajectory recrossing of the central barriers. These findings depend of course on the assumed potential energy surface, whose validity is uncertain. Furthermore the calculations of Hase and co-workers have uncertainties in the definition of the reaction coordinate and the treatment of zero point effects. Thus further tests of the validity of transition state theory are in order, and the kinetic isotope effects discussed in the present paper provide such tests.

Since recent experimental work on energy utilization in S_N2 reactions and energy disposal in the dissociation of ion-dipole complexes has been interpreted in terms of the applicability of statistical rate theories to S_N2 reaction rates, this work also deserves comment here. For example, Viggiano *et al.*[3b] found that when all degrees of freedom are not characterized by a single temperature, the rate constants are not strongly dependent on vibrational energy. This, however, is not directly relevant to the validity of transition state theory because transition state theory makes no prediction about the dependence of bimolecular rate constants on vibrational quantum numbers or translational energy. A similar situation occurs in unimolecular rate theory, and one requires added approximations[35] about exit channel interactions to predict the disposal of the total energy into particular modes, or—by microscopic reversibility—one requires extra assumptions about the interactions of reactants on the way to the transition state to make predictions about the utilization of various forms of energy.

Graul and Bowers[3e] have inferred non-RRKM dynamics in the dissociation of metastable ion-dipole complexes. Again it is relevant to note that we cannot infer whether the transition state assumption is valid at a tight activated complex by observation of product energy distributions.[35] Second, we note that it is not necessary for intermediate complexes to show equilibrium behavior for transition state theory to be valid for a low-pressure bimolecular process. A closely related point made by Graul and Bowers is that the internal energy and angular momentum distributions in the relatively long-lived metastable complexes are quite different from those in the nascent collision complexes. Graul and Bowers[3e] conclude that the thermal energy kinetics and the S_N2 activation energies are adequately modeled by statistical theories.

KIEs. In all cases, the calculations successfully predict that the kinetic isotope effects are inverse at 300 K (Table 7). For the reactions $Cl^- + CH_3Br$ and $Cl^- + CH_3I$ the calculated values are in reasonable agreement with the experiments, considering the difficulties of the experiments. However, the calculated KIE for the reaction $Br^- + CH_3I$ is quite different from the experimental value, with the calculated value 22−26% higher. In all cases, our calculations predict higher KIEs than the experiment.

It is also noted that in Table 7 the MP2/PTZ+ calculations give slightly higher KIEs than the MP2/PDZ+ calculations for the $Cl^- + CH_3Br$ reaction and give almost the same KIEs (within 1%) for the other two reactions. These tests give us confidence that the calculations are reasonably well converged with respect to the basis set size. The effects of removing diffuse d and f functions from the aug-cc-pVTZ set were checked by performing a calculation on the $Cl^- + CH_3Br$ reaction with the PTZ++ basis set. Compared to the MP2/PTZ+ calculation, the calculated energy of reaction (−6.0 kcal/mol) is 2.6 kcal/mol higher, and the calculated barrier height (−0.7 kcal/mol) is 0.3 kcal/mol higher. The KIE at 300 K obtained is 0.95 compared to 0.94 from the MP2/PTZ+ calculation. Thus it seems that the exclusion of the diffuse d and f functions from the aug-cc-pVTZ basis set does not affect the result significantly.

Since our KIE calculations on the $Br^- + CH_3I$ reaction yield results that are very different from the experimental ones, we

(35) (a) Herschbach, D. R. *Faraday Disscuss. Chem. Soc.* **1973**, *55*, 233. (b) Cheung, J. J.; McDonald, J. D.; Herschbach, D. R. *Faraday Disscuss. Chem. Soc.* **1973**, *55*, 377. (c) Marcus, R. A. *Faraday Disscuss. Chem. Soc.* **1973**, *55*, 379, 381.

performed an MP4/PDZ+ calculation including geometry optimization and calculation of the vibrational frequencies to check the convergence with respect to the level of electron correlation. Compared to the MP2/PDZ+ calculation, the calculated energy of reaction (−5.0 kcal/mol) is 0.5 kcal/mol higher, and the calculated barrier height is 1.3 kcal/mol lower. The KIE at 300 K obtained is 0.96 compared to 0.93 from the MP2/PDZ+ calculation. This might suggest that the frequency calculation, although well converged with respect to the size of the one-electron basis set, is not well converged with respect to the level of including correlation. However, since the KIE shifted farther from the experimental value when the higher level was used to calculate the frequencies, the discrepancy between theory and experiment is not resolved.

From Table 8 we see that the translational contributions to the KIEs are 1.01 in all three cases, and the rotational contributions are 1.23−1.24. While the translational and rotational contributions are "normal", the vibrational contributions are very "inverse". In all cases, the variational effects, i.e., the differences between the CVT rate constants and the TST rate constants, are found to be less than 4% for k_{ii} in the 200−1000 K temperature range, and the variational effects on the KIEs are found to be less than 0.5%. Thus the variational contribution η_{var} in eq 4 is essentially unity in this study. The capture rate contributions are also close to unity. Further analysis shows that the low-frequency-mode and high-frequency-mode contributions are "inverse" and the mid-frequency-mode contribution is "normal", which is consistent with earlier studies.[2j,11,12]

The inverse effect for high-frequency modes is due to the C−H stretches increasing 100−200 cm^{-1} as one proceeds from the reactants to the transition state. It is noted that the frequencies of the bending modes (except the transitional mode ν_7) decrease from the reactant to the transition state and this is the reason that the mid-frequency modes give a normal contribution to the KIEs. We see in Table 8 that every factor has a very similar value for all three reactions; these factors can therefore be viewed as typical of this type of gas-phase halide−methyl halide S_N2 reaction. It is also noted in Table 8 that the contributions from the mid-frequency modes are not well converged, and they are the major differences between different levels of calculations.

Anharmonicity. Since the KIE contributions from the translational and rotational motion can be estimated very accurately, the main uncertainty is from the vibrational contribution. The KIEs are very sensitive to the vibrational frequencies, and therefore anharmonicity could have significant effects on the results. However, in polyatomic systems it is very difficult to estimate anharmonic effects accurately, and the principal (i.e., intra-mode) anharmonicity often affects the partition functions in the opposite direction from the mode−mode coupling.[36] Nevertheless, the anharmonicity in the stretches is easier to deal with than that for the bending modes. In this study, we used two methods to estimate the effects of the anharmonicity of the stretching modes. In the first method, we applied the Morse I model,[37] which calculates the anharmonicity constant from the local dissociation energy and the harmonic frequency, to the four stretches in the systems (three C−H stretches and one C−X stretch for reactant, and three C−H stretches and one X−C−Y quasisymmetric stretch for the transition state). Using this method to estimate stretch anharmonicity, the rate constants at 300 K increase by less than 4.5% and the KIEs increase by less than 2%. The increase in the KIEs results exclusively from the C−H stretches, and this reflects the fact that the anharmonicity decreases the differences in the zero-point energies of these modes between the transition state and the reactant.

In the second method, we used the experimental[31] fundamental and harmonic frequencies to estimate the accurate zero-point energies, within the Morse model, of the three C−H stretching modes in the reactant. Then we replaced the calculated harmonic frequencies of these modes with effective frequencies that yield the correct zero-point energies harmonically, and we scaled the calculated harmonic frequencies of the three C−H stretching modes at the transition state by the ratio of the effective frequency to the calculated harmonic frequency at the reactant. The harmonic model is then used with these effective frequencies for all the modes in the rate constant calculations. This method effectively corrects the treatment of the C−H stretches both for anharmonicity and also for systematic errors in the *ab initio* harmonic frequencies. These corrections increase the rate constants at 300 K by less than 5.5%, and the KIEs are increased by less than 1.5%.

Since we only corrected the stretches, the above attempts to estimate the effect of anharmonicity treatment are not complete. However, they do show that the anharmonicity of the stretches does not affect the results significantly and does not reduce the disagreement with experiment.

Temperature Dependence of Rates. We now turn our attention to the temperature dependences of the rate constants. Usually the rate constant of a bimolecular reaction increases as temperature increases because an increase in temperature increases the fraction of collisions that have enough energy to overcome the energy barrier. In transition state theory, the positive temperature dependence of the rate constant is primarily due to the exponential term $\exp(-V^{\ddagger}/k_BT)$. However, the gas-phase S_N2 reactions studied here have negative barriers (as illustrated in Figure 1, the potential surface has an ion-dipole well in the entrance channel, followed by a saddle point, but the rise from the well to the saddle point is less than the well depth), and the calculated rate constants in Figures 2−4 show negative temperature dependences at lower temperatures, because of the $\exp(-V^{\ddagger}/k_BT)$ term, and negligible (or slightly positive) temperature dependence at higher temperatures, because of the balancing of the k_BT/h and $\exp(-V^{\ddagger}/k_BT)$ terms, with the vibrational partition functions also contributing to the positive temperature dependence. The temperature dependence of R^{CUS} is relatively small for slower reactions, and in the present study it changes by only 2% for the $Cl^- + CH_3Br$ and $Br^- + CH_3I$ reactions and by as much as 37% for the faster $Cl^- + CH_3I$ reaction in the 200−1000 K range. The temperature dependence of the rate constants has been measured only for the reactions of Cl^- with CH_3Br and CD_3Br. Figure 2 shows that the calculated results agree qualitatively with recent experiments in that the temperature dependence of k_H is negative below 500 K and is positive above this temperature.

As seen in Figures 2−4 the rate constants of the $Cl^- + CH_3I$ reaction show much stronger temperature dependence at lower temperatures than those for the other two reactions because of the more negative barrier, which can be correlated to the larger exoergicity of the reaction (see Table 5). It is interesting to characterize the temperature dependences quantitatively in conventional activation energy language. To do this we fit the rate constants calculated using the MP2/PTZ+ data to the Arrhenius form, $A\exp(-E_a/RT)$, at two temperatures, T_1 and T_2. Table 9 gives the resulting E_a values for $T_1 = 300$, $T_2 = 400$ and for $T_1 = 600$, $T_2 = 1000$. For the first pair of temperatures the E_a are all negative. This is apparent in Figures

(36) Isaacson, A. D.; Truhlar, D. G.; Scanlon, K.; Overend, J. *J. Chem. Phys.* **1981**, *75*, 3017.
(37) Garrett, B. C.; Truhlar, D. G. *J. Phys. Chem.* **1979**, *83*, 1079.

Table 9. Arrhenius Activation Energies

reaction	T_1 (K)	T_2 (K)	E_a (kcal/mol)
$Cl^- + CH_3Br$	300	400	−0.50
	600	1000	1.04
$Cl^- + CD_3Br$	300	400	−0.52
	600	1000	1.00
$Cl^- + CH_3I$	300	400	−1.61
	600	1000	−0.19
$Cl^- + CD_3I$	300	400	−1.64
	600	1000	−0.26
$Br^- + CH_3I$	300	400	−0.53
	600	1000	0.94
$Br^- + CD_3I$	300	400	−0.56
	600	1000	0.90

2−4 since in this temperature range the rate constants are all decreasing. For the second pair of temperatures E_a is negative for $Cl^- + CH_3I$ and positive for the other two reactions. This can be understood by noting that $Cl^- + CH_3I$ has a lower barrier, and the temperature dependence at this temperature range is still dominated by the $\exp(-V^{\ddagger}/k_BT)$ term, while for the other two reactions the temperature dependences are controlled by the k_BT/h term and the vibrational partition functions in this temperature range.

Rabini *et al.*[38] discussed the temperature dependence of the reaction rate in terms of the steric cone of reaction with increasing energy. This would indicate that the temperature dependence has a strong contribution from the doubly degenerate X···C−H bending (ν_7) partition functions. In this study we do find a strong temperature dependence contribution from the partition function of this mode, which is expected for the transitional modes, but this dependence is partially compensated by the bending modes, and, as always, the temperature dependence of the rate constants depends strongly on the barrier height.

Temperature Dependence of KIEs. The calculated KIEs for all these reactions are inverse at all temperatures studied and show a positive temperature dependence. As explained earlier, the temperature dependence is primarily due to the vibrational contribution, which can be further factored into contributions from the low-, mid-, and high-frequency vibrational normal modes. From Figures 6−8 we see that in these three reactions the low-frequency contributions are almost temperature independent, while the mid- and high-frequency contributions show negative and positive temperature dependences, respectively. The capture rate contributions are almost temperature independent (and very close to unity) except for the $Cl^- + CH_3I$ reaction at low temperatures. The combined effect is a small positive temperature dependence of the KIEs.

The present KIEs agree qualitatively with the available experimental and previous NDDO-SRP results[34] for the $Cl^- + CH_3Br$ as a function of T. Compared to the previous NDDO-SRP calculation[34] the present work gives more reliable geometries and vibrational frequencies for the reactant and the transition state, and this work predicts a smaller change in the KIE (0.91 to 0.95) than does the NDDO-SRP calculation (0.88 to 0.97) from 207 to 564 K. The only experimental[34] measurement of the temperature dependence of the KIEs does show positive temperature dependence but with big uncertainties in the absolute value of KIEs.[3b,34] Experimental data are not available for the other two reactions at temperatures other than 300 K.

Concluding Remarks

We have performed correlated extended-basis-set electronic structure calculations on the reactants and transition states of the gas-phase S_N2 reactions $Cl^- + CH_3Br$, $Cl^- + CH_3I$, and $Br^- + CH_3I$. The KIEs are calculated using the canonical unified statistical theory, and they are in reasonably good (but not perfect) agreement with experiment at 300 K for the first two reactions, but not for the $Br^- + CH_3I$ reaction. The calculated KIEs are inverse, and this is attributed to the vibrational contributions, in particular, the low- and high-frequency mode contributions. The temperature dependences of the KIEs are also calculated and are in qualitative agreement with available experimental data. The positive temperature dependences of the KIEs are attributed to the combined effect of the mid- and high-frequency mode contributions.

In light of recent work that illustrated nonstatistical aspects of these ion−molecule reactions, the semiquantitative agreement of theory and experiment for the reactions $Cl^- + CH_3Br$ and $Cl^- + CH_3I$ KIEs might be considered surprisingly good. On the other hand, in light of the general high quantitative predictive ability of variational transition state theory for many other reaction rates, the lack of fully quantitative agreement with experiment for these reactions and the even larger discrepancies for $Br^- + CH_3I$ might be considered equally disturbing. More experimental work would be valuable to test the predictions of these theoretical calculations. In particular it is important for our fundamental understanding of this widely studied class of reactions to understand why the calculated kinetic isotope effects are larger than experimental values by up to 26%. Is it due to a breakdown of generalized transition state theory—either associated with the nonstatistical behavior previously pointed out or due to some other aspect of the reactions? Or is it due to slow convergence of the electronic structure calculations, anharmonicity, or the difficulty of the experiments? Time will tell, and we anticipate that this class of reactions will continue to provide the standard for testing our fundamental understanding of gas-phase ion chemistry.

Appendix

In the course of this work, we calculated the kinetic isotope effect by conventional transition state theory with a large number of basis sets at the Hartree−Fock and MP2 levels. These results could be useful to other workers contemplating the treatment of more complicated reactions, and so they are presented in the supporting information.

Acknowledgment. This work was supported in part by the U.S. Department of Energy, Office of Basic Energy Sciences.

Supporting Information Available: Tables giving geometries and frequencies of reactants and transition states, SRP parameters, basis set sizes, and vibrational frequencies and kinetic isotope effects calculated at many levels of electronic structure theory other than those presented in the published part of this article (17 pages). This material is contained in many libraries on microfiche, immediately follows this article in the microfilm version of the journal, can be ordered from the ACS, and can be downloaded from the Internet; see any current masthead page for ordering information and Internet access instructions.

JA951547U

(38) Rabani, E.; Charutz, D. M.; Levine, R. D. *J. Phys. Chem.* **1991**, *95*, 10551.